

Test Results of a 1.5MW High Speed Motor-Generator in a Pressurized CO₂ Environment

Jason D. Miller
Engineering Manager
Echogen Power Systems, Inc.
Akron, Ohio

Timothy J. Held
Chief Technology Officer
Echogen Power Systems, Inc.
Akron, Ohio

Kyle Sedlacko
Senior Systems Engineer
Echogen Power Systems, Inc.
Akron, Ohio

Jared Hubach
Engineering Intern
Echogen Power Systems, Inc.
Akron, Ohio

Roberto Zullo
Director/Principal Engineer
Samnium Aerospace
Cleveland, Ohio

ABSTRACT

The high-power density of supercritical carbon dioxide turbomachinery can be most fully exploited by utilizing a directly-coupled generator. To eliminate leakage of the working fluid through external shaft seals, the generator will operate in a pressurized CO₂ environment. This arrangement poses several unique design challenges. Windage at high rotational speed at elevated fluid density can result in high power losses, as well as localized heating within the enclosed cavity. This windage heating, in addition to all electrical losses, must be removed from a compact physical volume. Thus, generator cooling design is critical to effective operation, and accurate thermal modeling is critical to effective cooling design. In this study, two 1.5MW permanent magnet generators are mechanically coupled and operated, with one generator energized as a motor to drive the second generator. Both generators operate in a pressurized CO₂ environment, using circulated CO₂ as the rotor coolant. Generator speed and CO₂ pressure are varied and the windage and thermal results are compared to theory and detailed CFD modeling.

INTRODUCTION

Because of the high-power density of supercritical carbon dioxide (sCO₂) turbomachinery, sCO₂ power cycles have great potential for use in applications where space is highly constrained. This is especially true in marine environments. GE-Marine (GE) commissioned Echogen Power Systems to design and fabricate a 1.5 MW_e heat engine for use as a bottoming cycle on high and medium speed diesel engines and gas turbines for ship board applications. The requirements for successful deployment include a leak free system, as the ability to store and transport carbon dioxide (CO₂) for make-up is limited in marine applications. This precluded the use of a more standard turbine-gearbox-generator power train arrangement due to the shaft seal on the turbine. A better option for this application is to encapsulate a high speed permanent magnet alternator in the working fluid, allowing for a leak free option.

Echogen worked Elektromaschinen und Antriebe (e-a) to design and build a high speed permanent magnet alternator, to spin at 25,000 RPM at a power of 1.5 MW_e. This speed and power combination represents significant design challenges for the both the alternator design as well as the thermal management (cooling) system. Due to the high degree of risk associated with this aggressive design, Echogen chose to operate a “back-to-back” test of an identical pair of alternators, with one operating as the driver (motor), and the other as the load (alternator), as shown in Figure 1.

For this test, the two machines were connected by a custom “dog-bone” spline shaft and utilized oil-lubricated ball bearings. The power electronics system was reconfigured to convert electrical power from the machine operating as an alternator to a DC bus. The DC bus power was then converted back to high frequency AC power to operate the motor. The difference in generated power and required power for the motor was compensated by a separate DC power supply operating off the local grid supply.

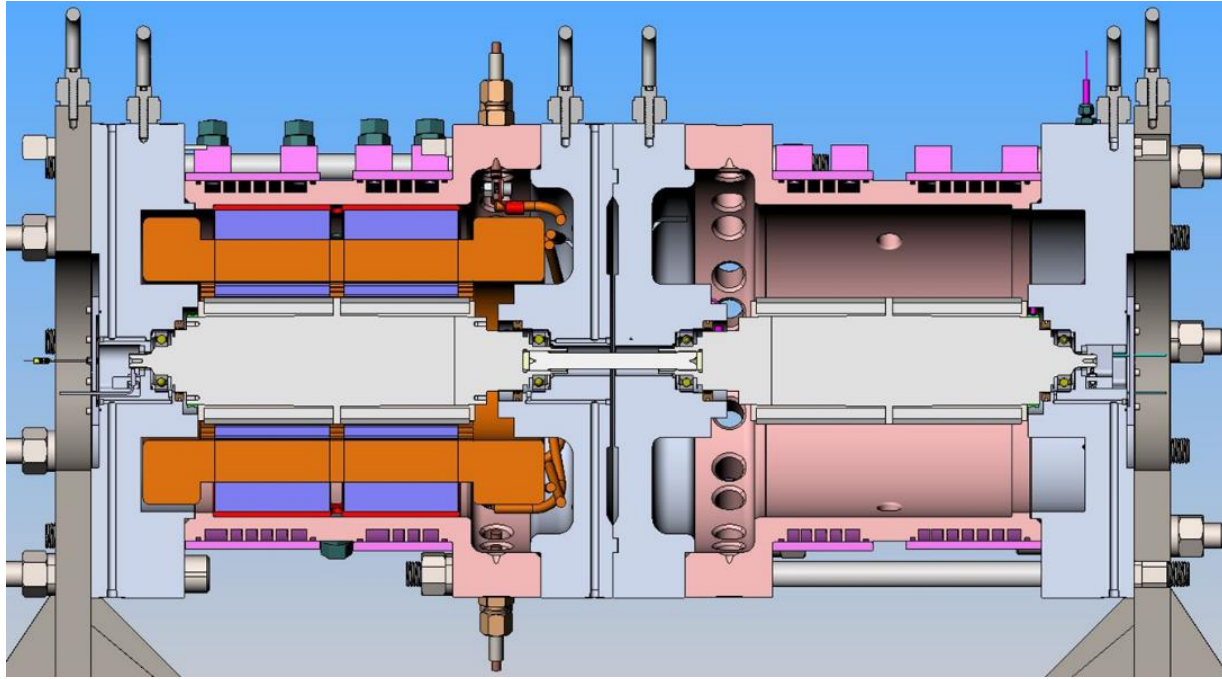


Figure 1 High speed alternator test configuration - Right side shown with stator.

ALTERNATOR THERMAL MANAGEMENT DESIGN

The encapsulated alternator configuration requires careful cooling design. The as-tested configuration, shown in Figure 2, includes both CO₂ and external water cooling, with a complex flow path for both fluids, as shown in Figure 3. Heat is generated in the high-speed alternator (HSA) through the following mechanisms: windage heating due to the aerodynamic drag between the rotor and stator, copper (winding resistance and inductance) and lamination (iron eddy current) losses in the stator, magnet (eddy current) losses in the rotor and ball bearing losses. The copper, lamination, rotor, and magnet loss estimates were supplied by e+a at the steady-state design condition of the machine. A summary of internal HSA and bearing losses is shown in Table 1.

Table 1 Estimated heat loads for the high-speed alternator and ball bearings

Heating Source	Load (kW)
Copper (25,000 RPM and 1.5 MWe)	10.00
Rotor (25,000 RPM)	0.65
Lamination (25,000 RPM)	15.00
Magnet (25,000 RPM)	0.55
Ball Bearing (25,000 RPM)	0.10

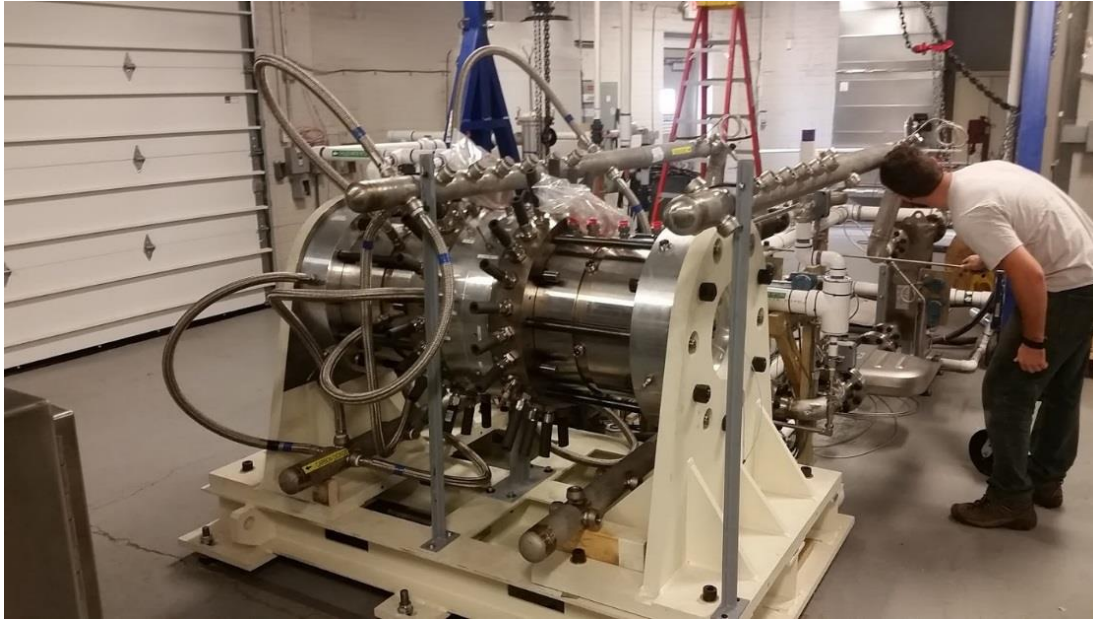


Figure 2 High speed alternator test stand

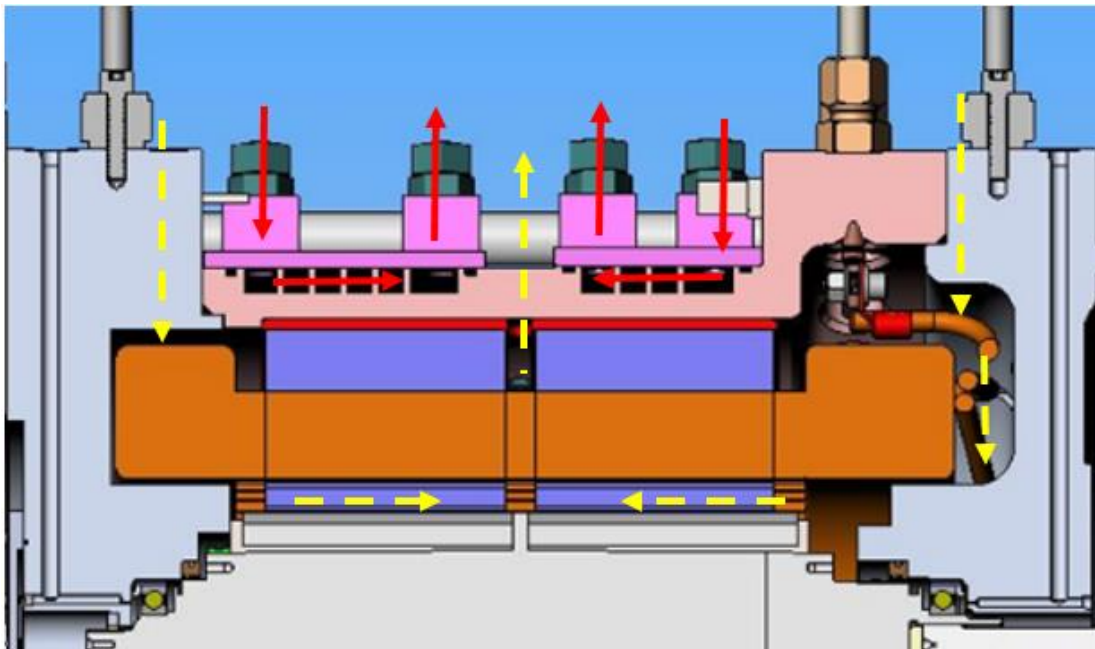


Figure 3 High speed alternator test section, CO₂ (yellow dashed line) and water (red solid line) cooling flow paths

One of the significant challenges in the encapsulated design is the management of aerodynamic drag (windage). To first order, windage is expected to be proportional to fluid density and to the cube of rotational speed. If the alternator cavity density reached levels characteristic of the “low-side” pressure of the sCO₂ cycle, windage losses would overwhelm the cooling capacity of the system, and drastically degrade the system performance. To alleviate this effect, Echogen is using a semi-sealed alternator cavity with a pressure control system that maintains the cavity pressure at approximately 0.7 MPa. This pressure was chosen to balance the achievable alternator cooling flow and windage losses.

Windage losses were estimated using three methods. Simplified 1-D fluid models using the methods described by Saari [1] and Hamm [2] were first used to bound the cooling requirements for the design of the heat rejection system. The results of the calculations and boundary conditions are summarized in Table 2.

Table 2 Design parameters used for Hamm and Saari windage heating calculations

Rotor radius (mm)	88
Stator radius (mm)	90
Rotor length (mm)	381
CO2 density (kg/m ³)	14.78
CO2 viscosity (10 ⁻⁶ Pa-s)	18.37
Rotor speed (RPM)	25,000
Hamm windage estimate (kW)	28.3
Saari windage estimate (kW)	41.5

From this analysis, a target CO2 cooling flow rate of 0.65 kg/s was selected to maintain rotor and stator temperatures within an acceptable range, while assuming the more conservative windage estimate of 41.5 kW.

A detailed 3-D Computational Fluid Dynamics (CFD) and thermal simulation of the alternator cooling system was created for final design and analysis. The model was created in ANSYS-CFX 16.0, used REFPROP values of CO2 thermodynamic and transport properties and utilized conjugate heat transfer methods to define the fluid-solid interactions. The physical domain, solid and fluid meshes are shown in Figure 4 and 5.

The inlet and boundary conditions for the CO2 and water cooling and the windage loss calculated through CFD is shown in Table 3, and the imposed heat loads due to the HSA internal losses for the final analysis are listed in Table 1. Note the ball bearing losses were not included in the CFD model due to their small magnitude and position outside the computational domain. Windage was calculated directly by the CFD simulation based on an assumed rotor surface roughness characteristic of fiber-wound rotors. It should be noted here the simplified model for windage proposed by Saari agrees well with the results of the full 3-D CFD simulation, while the Hamm model significantly under-predicts the simulated value.

Table 3 Boundary conditions used for 3-D CFD analysis

CO2 Inlet Temperature (°C) / Inlet Pressure (MPa)	50 / .9950
Total CO2 Mass Flow Rate (kg/s)	0.65
Cooling Water Temperature (°C) / Pressure (MPa)	38 / 0.2
Cooling Water Flow Rate (kg/s)	0.95
Windage Loss Calculated (kW)	44.912

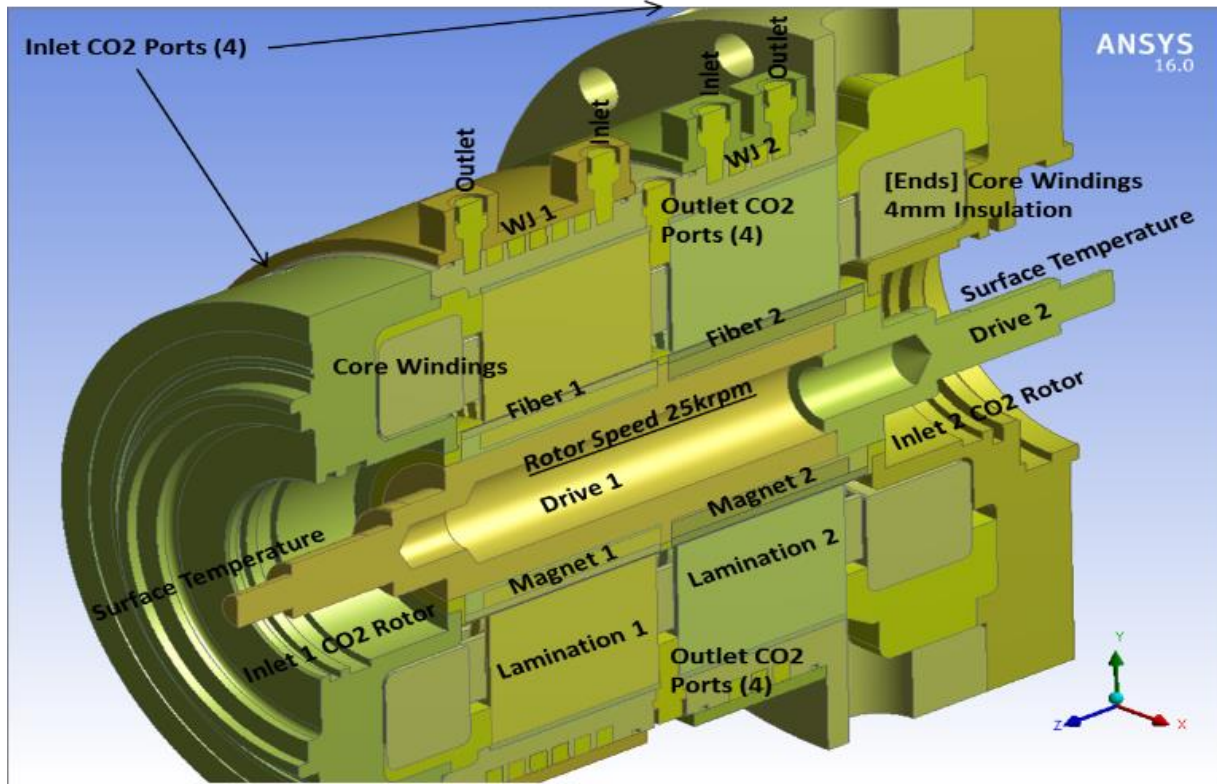


Figure 4 Physical domain used for 3-D CFD simulation

The resulting temperature field prediction is shown in Figure 6 along with point temperature measurements that were made during testing at an approximately equivalent operating condition to that used in the analysis. The temperature measurements were adjusted to compensate for the lower coolant inlet temperature used during the test relative to the values used in the CFD analysis. In general, the agreement is quite good, within approximately 10°C for all measured points.

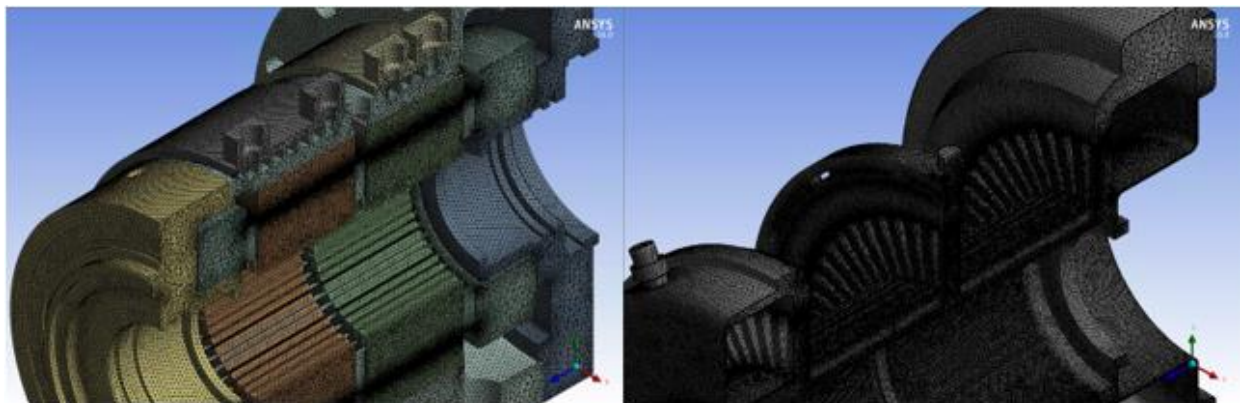


Figure 5 Solid and fluid meshes used in 3-D CFD simulation

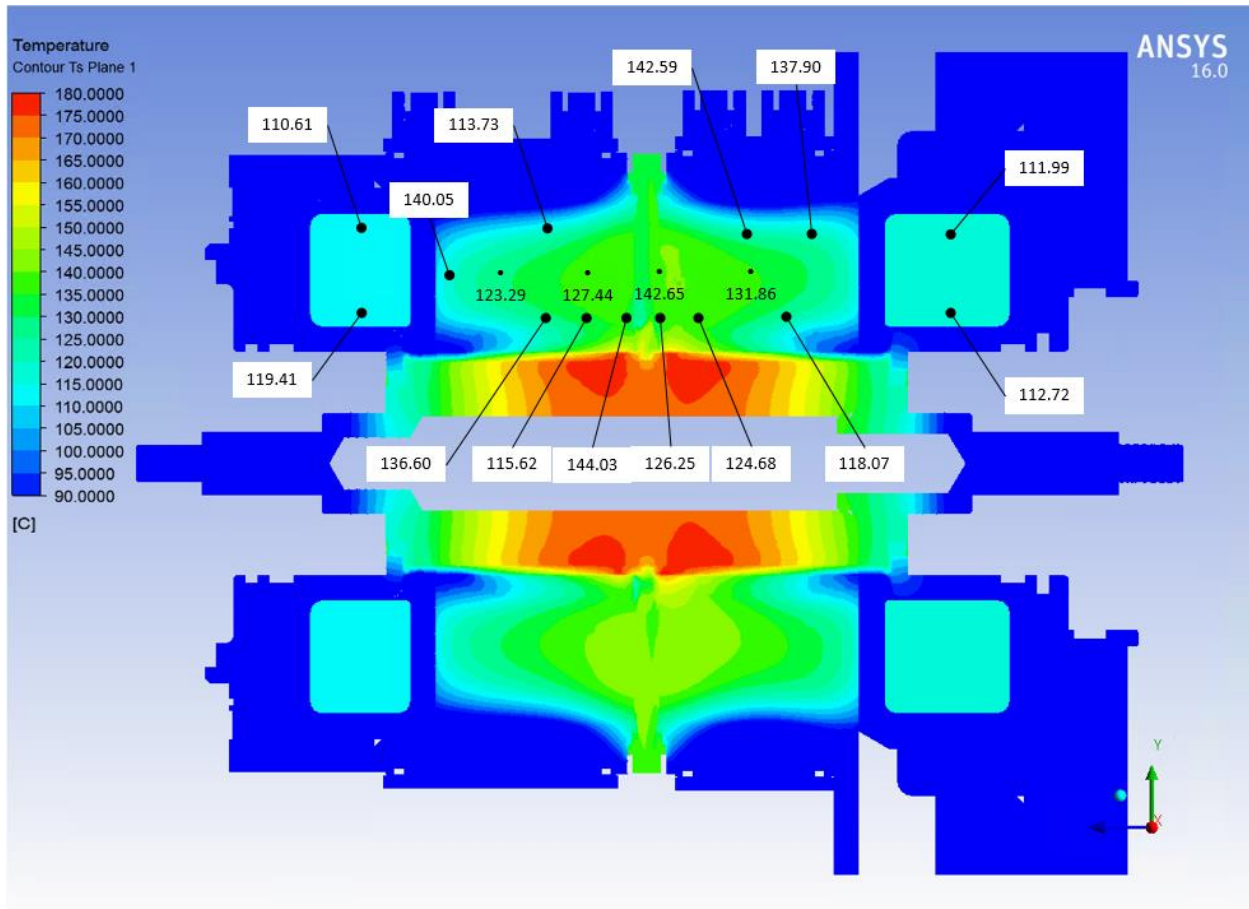


Figure 6 Resulting temperature field of the CFD analysis with measured temperature points superimposed

COOLING SYSTEM DESIGN

The alternator cooling system consists of two fluid loops. The first provides a recirculating flow of CO₂ at a controlled pressure to provide internal cooling of the rotor, alternator end turns, and inner surfaces of the stator. The second loop provides water to the outer surface of the alternator to cool the outer surfaces of the stator. In addition, the water loop also extracts the accumulated heat from the recirculating CO₂ and provides cooling for the power electronics and the bearing lubrication oil. Details of each loop are documented and described below

CO₂ Cooling Loop

The CO₂ cooling loop shown in Figure 7 supplies CO₂ to the both HSAs. Because the machines are run in a back-to-back configuration, two identical cooling loops are provided. Each loop is comprised of a blower to recirculate CO₂ through the alternator, a heat exchanger to transfer heat to the water cooling loop, and a flow meter. The blowers supply 0.6-0.65 kg/s of CO₂ directly to each HSA, entering near the alternator winding end turns and exiting near the center of each machine through a passage provided in the center of the stator lamination stack.

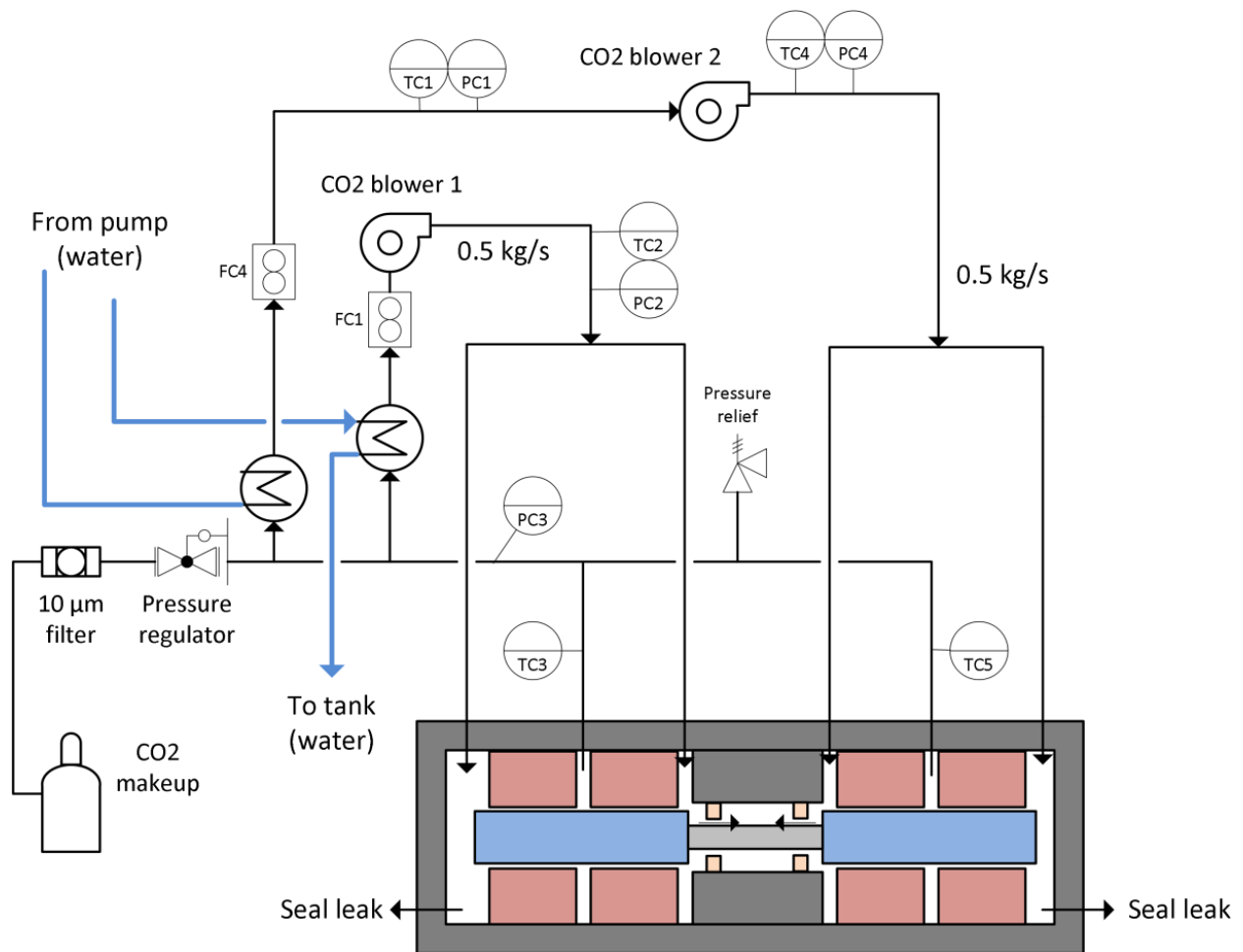


Figure 7 Alternator Test - CO₂ cooling loop process flow diagram

CO₂ lost through the labyrinth seals located at both ends of each machine is replenished from a liquid CO₂ storage tank located outside the building. The liquid CO₂ is fed through a 10-micron filter, heated and evaporated, and passed through a pressure regulating valve and measured with a Coriolis flow meter. The pressure regulating valve is used to set the operating pressure for the HSAs. For all testing to date, the CO₂ make-up supply was regulated to approximately 0.7 MPa at 45°C. The make-up CO₂ is mixed into the return header of the CO₂ discharge of the machines.

Water cooling loop

The cooling water loop shown in Figure 8 is designed to remove heat directly from the HSA, power electronics (PE), CO₂ blowers, lubrication oil for the high-speed ball bearings, and from the heated CO₂ leaving the HSA. The hot water rejects heat to the environment through an evaporative cooling tower and returned to the tank for recirculation. Temperature, pressure and flow instrumentation was provided as indicated in Figure 8 below.

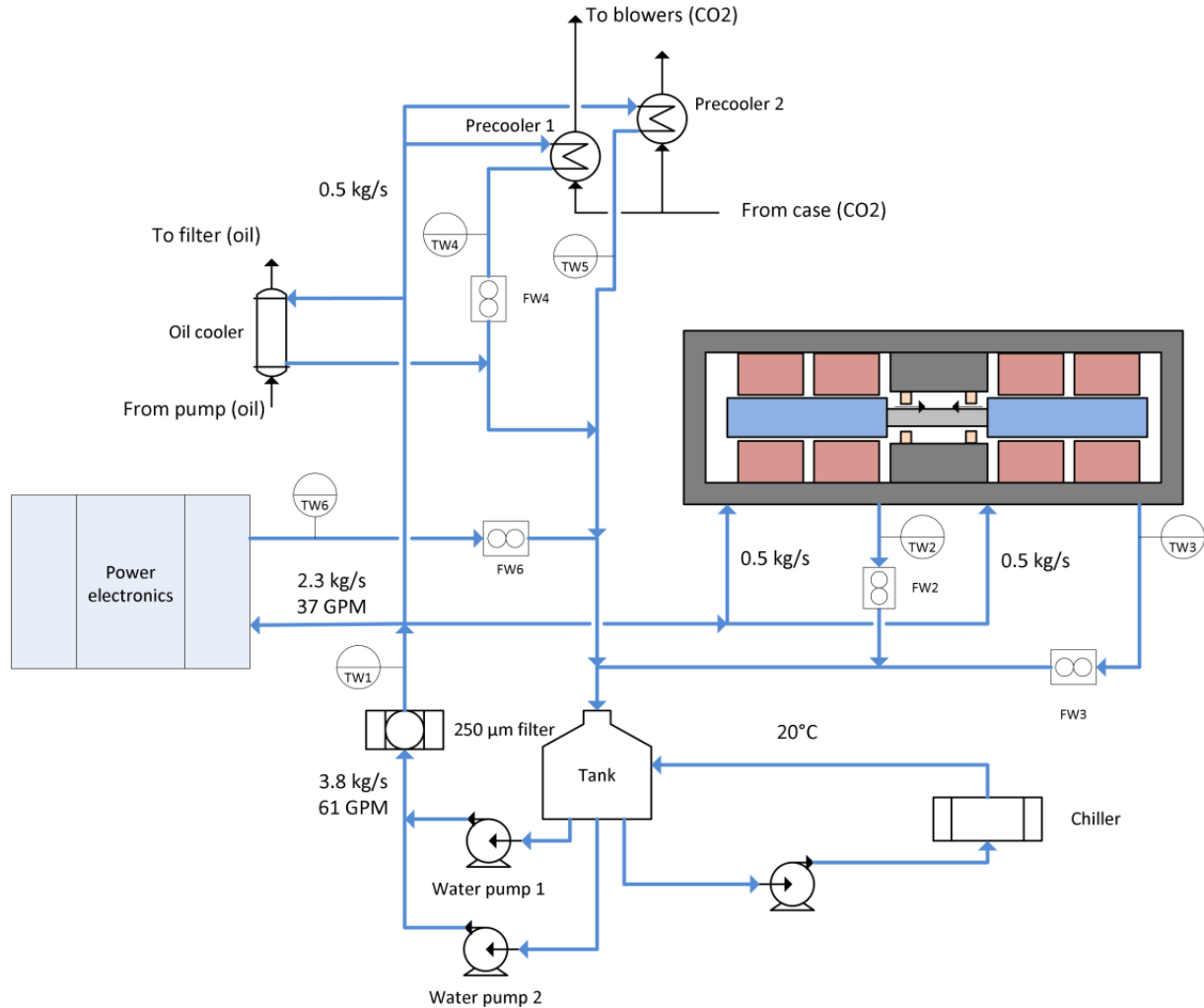


Figure 8 Alternator Test - Water cooling loop process flow diagram

TESTING RESULTS

Using the pressure, temperature and flow measurements from the CO₂ and water cooling loops the total heat generated in the HSA was calculated, using the HSA case as the control volume boundary. Heat picked up by the CO₂ and water cooling loops was calculated using the measured inlet and outlet conditions of the respective loops. While the leakage discharge state was not measured directly, for the purposes of the heat balance it was assumed it was discharged as the same pressure and temperature as the primary CO₂ discharge header. The complete CO₂ and water mass and heat balance is shown in Equation Set 1.

Equation Set 1: High speed alternator heat and mass balance equations

$$Q_{CO_2} = w_{CO_2in} * (h_{CO_2out} - h_{CO_2in}) - w_{leak} * h_{CO_2out}$$

$$Q_{H_2O} = w_{H_2O} * (h_{H_2Oout} - h_{H_2Oin})$$

$$Q_{Tot} = Q_{CO_2} + Q_{H_2O}$$

Based on the results of the CFD modeling, simplified windage calculations and the assumed scaling relationships for the alternator and bearing losses the predicted heat generated for comparison with the experimental values are shown in Equation Set 2. The reference conditions (25,000 RPM, 14.78 kg/m³,

and 1.5 MWe) are based on the design values for the machine, and the multipliers are the predicted design point loads.

The copper losses scale with rotor speed and alternator power, lamination and magnet losses scale only with speed. The ball bearing losses at full speed supplied by the manufacturer this lose scales solely with speed. The windage scaling law followed the same scaling this is in the Saari and Hamm calculations, in that windage heat generated scales roughly with rotor speed cubed and linearly with density.

Equation Set 2: Predictive scaling relationships for windage and generator losses

$$Q_{Windage} = 41.54 * \left(\frac{N_{act}}{25,000 \text{ RPM}} \right)^3 * \left(\frac{\rho}{14.78 \text{ kg/m}^3} \right) \text{ kW}$$

$$Q_{Copper} = 10 * \left(\frac{N_{act}}{25,000 \text{ RPM}} \right) * \left(\frac{P_{HSA}}{1.5 \text{ MWe}} \right) \text{ kW}$$

$$Q_{Laminations} = 15 * \left(\frac{N_{act}}{25,000 \text{ RPM}} \right) \text{ kW}$$

$$Q_{Magnets} = 0.55 * \left(\frac{N_{act}}{25,000 \text{ RPM}} \right) \text{ kW}$$

$$Q_{Bearing} = 0.1 * \left(\frac{N_{act}}{25,000 \text{ RPM}} \right) \text{ kW}$$

$$Q_{Tot_{pred}} = Q_{Windage} + Q_{Copper} + Q_{Laminations} + Q_{Magnet} + Q_{Bearing}$$

Due to the large thermal mass of the HSA, it is important to only compare the model to data collected after the thermal lag or heat up time of the HSA has been corrected for. Figure 9 shows a time series plot of the measured and predicted generator losses, current generated and speed for a typical start and run of the HSA. An approximately 300 second lag, as noted, is present between the measured and predicted heat generation from when the machine is accelerated to speed and current is generated. This represents the time required for HSA to heat to a point in which the heat being generated through windage and internal losses is no longer being used to heat the large thermal mass of the HSA, but is being captured by the cooling fluids. Therefore, only data from conditions where the alternator had maintained steady-state operation for 300 seconds were used in the analysis.

Results comparing the predicted and experimental values of total windage and heat generated in the alternator are shown in Figure 10. The redline shown has a slope of 1 and represents what would be a perfect fit. Points lying above the line would under predict, while points below the line over predict. The data points used for comparison are noted in Figure 9, with slight variations of speed and current (power) accounting for the variation in heat generated. The only difference between the three predictions presented is in the windage model used, and each of the predictive windage models are shown separately in Figure 10. It can be seen that the Hamm model significantly under predicts when compared against the experimental data. For a measured loss of 38 kW_t, the Hamm model predicts between 30.5 kW_t to 31.5 kW_t at the same condition. The CFD and Saari models show good agreement with the measured data, with the CFD model slightly overpredicting and the Saari model slightly underpredicting.

The results show that a full 3D CFD analysis is the best prediction of the windage heating, with a standard deviation of the differences between model and experimental data of 1.63 kW and a mean difference of -0.54 kW. The Saari model has a standard deviation of the difference between model and data of 1.75 kW and mean of 1.17 kW, and the Hamm model had a standard deviation of 2.24 kW with a mean of 7.69 kW.

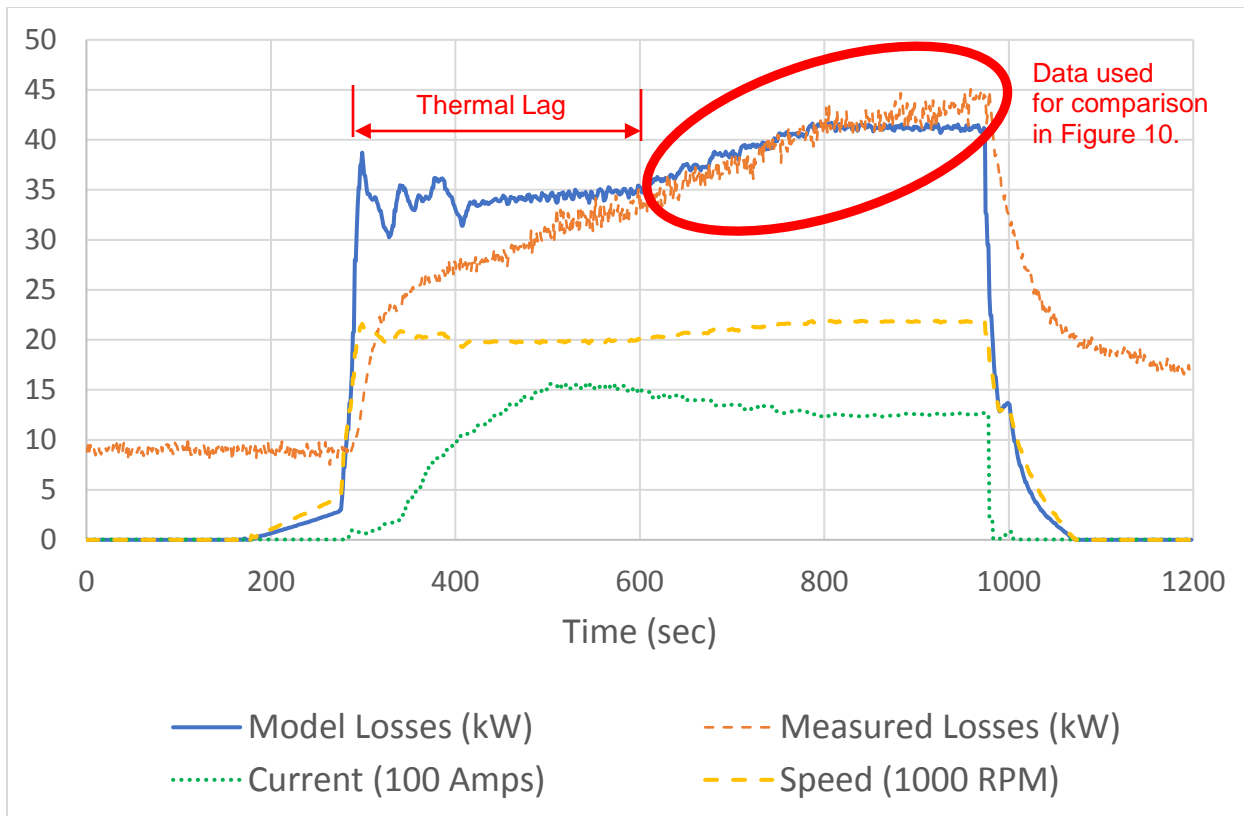


Figure 9 Typical alternator run showing the thermal time lag of the alternator as current and speed are increased

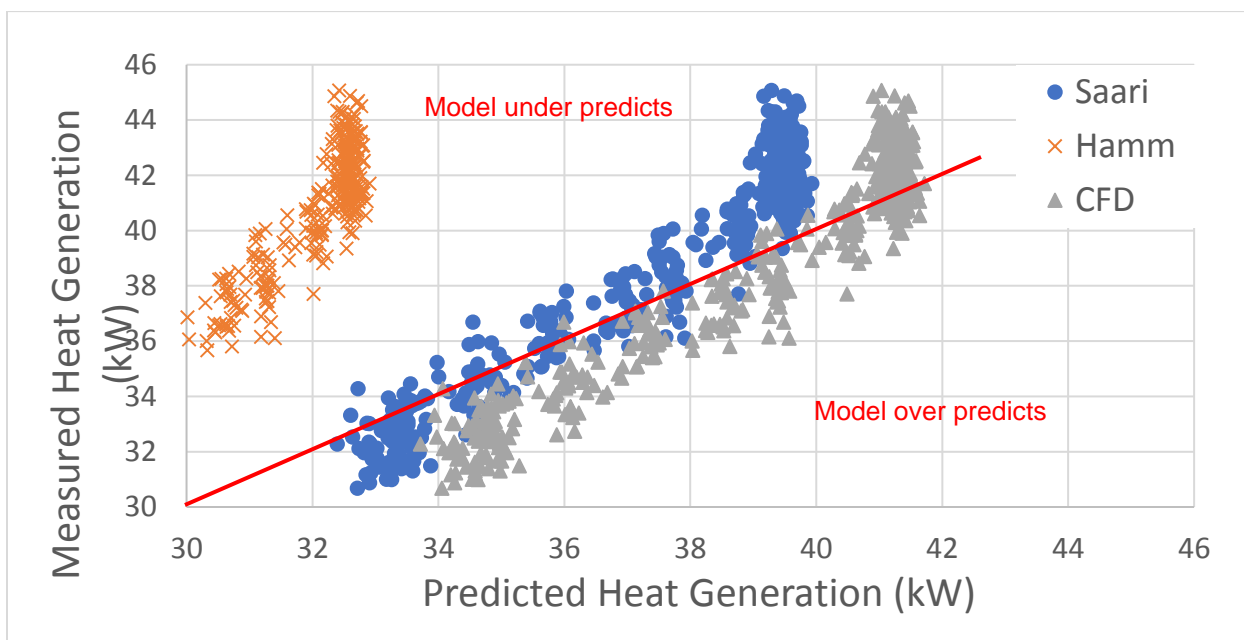


Figure 10 Comparison of alternator and windage heat generation predictions for the windage models against experimental data

CONCLUSIONS

A high-speed alternator was operated in a pressurized CO₂ environment. A test in which two identical machines were put back to back with one acting a generator and one acting as a motor was completed to verify operation of the high-speed alternator and thermal management systems and to validate heat generation predictions. Experimental data was taken to determine the heat generated in the alternator through internal losses and windage heating. This data was compared to predictions based on Saari and Hamm windage models as well as a full 3-D CFD prediction of windage heating. It was found the CFD and Saari predictions most closely estimated the windage heating and could be used for design predictions. The CFD model slightly underpredicted while the Saari model slightly overpredicted. The Hamm model under estimated the actual windage heat load significantly and should not be used.

REFERENCES

- [1] Saari, J. "Thermal Analysis of High-speed Induction Machines", Polytechnica Scandinavica, Electric Engineering Series No. 90, 1998
- [2] Hamm, H. W. "Determining Fluid Friction or Windage of Rotating Discs", Allis-Chalmers Electrical Review, Fourth Quarter, 1962